Journal of Clinical Immunology (2025) 45:85
https://doi.org/10.1007/s10875-025-01877-z

RESEARCH

DOCK2 Deficiency and GATA2 Haploinsufficiency Can Underlie Critical Coronavirus Disease 2019 (COVID-19) Pneumonia

Sajjad Biglari[1] · Leila Youssefian[2] · Mohammad Amin Tabatabaiefar[1] · Amir Hossein Saeidian[3,4] · Bahareh Abtahi-Naeini[5,6] · Erfan Khorram[7] · Roya Sherkat[8] · Atefeh Sohanforooshan Moghaddam[9] · Fatemeh Mohaghegh[10] · Maziyar Rahimi[11] · Hamid Rahimi[12] · Sharareh Babaei[13] · Mohammad Shahrooei[14,15] · Nikoo Mozafari[16] · Shirin Zaresharifi[16] · Fatemeh Vahidnezhad[17] · Vida Homayouni[8] · Lam C. Tsoi[18] · Johann E. Gudjonsson[18] · Hakon Hakonarson[3,19,20] · Jean-Laurent Casanova[21,22,23,24,25] · Emmanuelle Jouanguy[21,22,23] · Vivien Béziat[21,22,23] · Qian Zhang[21,22,23] · Aurélie Cobat[21,22,23] · Hassan Vahidnezhad[3,19,20,26]

Received: 13 March 2024 / Accepted: 16 March 2025

Abstract

The life-threatening coronavirus disease 2019 (COVID-19) affects about 1 in 1,000 healthy people under 50 without underlying conditions. Among patients with critical COVID-19 pneumonia, rare germline variants at genes controlling type I IFN immunity have been reported in up to 5% of patients. Causal etiologies in 80–85% of cases are still unknown. We analyzed two families with hypoxemic COVID-19 pneumonia for known single-gene inborn errors of immunity. In Family 1, two siblings with critical COVID-19 were homozygous for a *DOCK2* variant, c.3624+5G>A. DOCK2 deficiency is a known T-cell disorder underlying severe viral diseases. The variant resulted in skipping exon 35, which was predicted to produce a frameshift truncated protein (p.L1157Ifs*12). The proband showed markedly decreased blood CD4 T-helper cell counts, impaired T lymphocyte transformation test, and increased serum IgG, IgA, and IgE levels, as documented in other DOCK2-deficient patients. In Family 2, the proband had lethal COVID-19 and HPV-2-associated multiple recalcitrant warts. She was heterozygous for a deletion in *GATA2*:c.1075_1102del28, p.W360Sfs*18. GATA2 haploinsufficiency is a known cause of severe viral diseases due to a lack of plasmacytoid dendritic cell (pDC) development. The proband had monocytopenia and a lack of circulating pDCs, as reported in other patients with GATA2 haploinsufficiency. Overall, both DOCK2 deficiency and GATA2 haploinsufficiency are associated with critical and often fatal COVID-19 pneumonia.

Keywords DOCK2 deficiency · GATA2 haploinsufficiency · Inborn Errors of Immunity · Lymphocytic vasculopathy · Human papillomavirus · COVID-19

Abbreviations

ACMG	American College of Medical Genetics and Genomics
AD	Autosomal dominant
AOM	Acute otitis media
AR	Autosomal recessive
ARDS	Acute respiratory distress syndrome
ASD	Atrial septal defect
BCG	Bacillus Calmette–Guérin
CADD	Combined annotation-dependent depletion
CMPA	Cow's milk protein allergy
COM	Chronic otitis media
COVID-19	Coronavirus disease 2019
CID	Combined immunodeficiency
CMV	Congenital cytomegalovirus
CT	Computer tomography
DHR	DOCK homology region domain
DOCK2	Dedicator of cytokinesis 2
EBV	Epstein-Barr Virus
GATK	Genome analysis toolkit
GEF	Guanine nucleotide-exchange factor
GS	Genome sequencing
GWAS	Genome-wide association study association
Ig	Immunoglobulin
HC	Healthy controls
HGMD	Human Gene Mutation Database

Sajjad Biglari and Leila Youssefian these authors contributed equally.

Extended author information available on the last page of the article

Published online: 28 March 2025

HLH	Hemophagocytic lymphohistiocytosis
HPV	Human papillomavirus
HSCT	Hematopoietic stem cell transplantation
ICU	Intensive care unit
IEI	Inborn errors of immunity
ES	Exome sequencing
IUIS	International Union of Immunological Societies
IVIg	Intravenous immunoglobulin
LTT	Lymphocyte transformation test
MAF	Minor allele frequency
MIS-C	Multisystem inflammatory syndrome in children
ND	Not Determined
NICU	Neonatal intensive care unit
NGS	Next-generation sequencing
NK	Natural Killer
PBMCs	Peripheral blood mononuclear cells
PBS	Phosphate-buffered saline
PDCs	Plasmacytoid dendritic cells
PHA	Phytohemagglutinin
RECs	Respiratory epithelial cell
PICU	Pediatric intensive care unit
RNA-seq	RNA sequencing
ROH	Runs of homozygosity
ROS	Reactive oxygen species
RT-PCR	Real-time reverse transcription–PCR
SCID	Severe combined immunodeficiency
SARS-CoV2	Severe acute respiratory syndrome-related coronavirus 2
SNP	Single nucleotide polymorphism
SNV	Single nucleotide variant
SD	Standard deviation
SI	Stimulation index
TCR	T-cell receptor
VCF	Variant Call Format
WHO	World Health Organization
XLR	X-linked recessive

Introduction

Infection with severe acute respiratory syndrome-related coronavirus 2 (SARS-CoV2) can be asymptomatic in 40% of cases, underlie benign upper respiratory tract disease in another 40% of cases, cause moderate non-hypoxaemic pneumonia in 10% of cases, cause hypoxemic pneumonia necessitating hospitalization for oxygen therapy in 7% of cases, or lead to critical pneumonia necessitating intensive care in 3% of cases. The latter life-threatening disease probably affects fewer than 1 in 1,000 infected people under the age of 50 who do not have underlying conditions. Among critical coronavirus disease 2019 (COVID-19) pneumonia, rare germline sequence variants at genes controlling type I IFN immunity have been reported in 1%–5% of patients. Additionally, 15% of patients may develop critical COVID-19 pneumonia due to autoantibodies against type I IFN, a phenocopy of single-gene inborn errors of immunity (IEI) of type I IFN. Causal etiologies in at least 80–85% of cases are still unknown [1–5].

Several host genetic studies, including genome-wide association studies (GWAS) and unbiased and hypothesis-free next-generation sequencing (NGS) approaches, have contributed to understanding the roles of host genetics in infection susceptibility and COVID-19 disease severity, explaining which genetic factors make some individuals more susceptible to SARS-CoV-2 infection and why others develop severe symptoms. GWAS-identified genes linked to infection susceptibility and disease severity include *TLR7*, *OAS1*, *TYK2*, *ABO*, *ACE2*, and *DOCK2* [6, 7].

Additionally, NGS approaches for finding causal germline sequence variants in small numbers of patients with life-threatening COVID-19 pneumonia discovered autosomal recessive (AR) mutations in *IRAK4, MYD88, TYK2, STAT2, TBK1, IRF7, IRF9,* and *IFNAR1*, autosomal dominant (AD) mutations in *TLR3, TRIF, UNC93B, TBK1, IRF7,* and *IFNAR1, IRF3, IFNAR2,* and X-linked recessive mutations in *TLR7.* Collectively, these monogenic studies highlighted the roles of TLR-7/TLR3-dependent type I and/or III IFN immunity in immunity to SARS-CoV-2 infection [1–4, 8–10].

We hypothesize that other known or unknown single-gene IEI underlie critical pneumonia or life-threatening COVID-19 in at least some of these patients. We investigated three IEI patients who developed severe COVID-19 pneumonia and ultimately succumbed to complications from COVID-19. Our exome sequencing studies identified causal pathogenic variants in *DOCK2* or *GATA2* in Family 1 and Family 2, respectively, highlighting the genetic factors that may contribute to fatal COVID-19 outcomes in these cases.

Methods

Patient Data

This study was approved by the Institutional Review Board of the Isfahan University of Medical Sciences of Iran (IR.MUI.MED.REC.1401.255). Patient 3 and the parents of patients 1 and 2 gave written informed consent to participate in the research and to publish their images.

Exome Sequencing and in Silico *Analyses*

The DNA of the proband was isolated from peripheral blood cells using the salting-out procedure. Exome sequencing

(ES) was conducted in paired-end mode using 150 base-pair reads on the Illumina NovaSeq platform. For coding exons, the average coverage was 100. The output reads were aligned to version GRCh38 of the human genome. To identify PCR duplicates, we utilized Picard Tools software. We employed the genome analysis toolkit (GATK) for base-quality score recalibration and variant calling. Annotate Variation software was used to annotate the resulting list of variations. To detect the pathogenic variants, a multiple-step bioinformatics analysis was used [11, 12].

Whole-Transcriptome Sequencing by RNA-Seq

TRIzol® was used to isolate RNA from a 3-mm whole-skin biopsy of lesional tissue and normal-appearing adjacent skin to initiate RNA-Seq. Sequencing was performed using 100 nanograms of total RNA. Following the manufacturer's instructions, sequencing was conducted with the TruSeq Stranded Total RNA Kit (Illumina). The mRNA capture, library preparation at 4 nM concentration, barcoding, and sequencing on an Illumina Nexseq500 machine were carried out following standard procedures, and the results were saved in FASTQ format. Using the GRCh38 human reference genome and GENCODE V27 annotations, STAR-2pass (v. 2.5.3a) was utilized to perform alignment and mapping [13–15].

Viral Detection

Our recently developed in-house RNA-Seq application was utilized to explore the skin virome, including 926 different viruses, including 441 types of HPV, and identify the underlying viral determinant of a skin lesion by NGS-based detection [16, 17].

Co-Segregation and RT-PCR

To confirm and explore the segregation of the candidate variants in affected individuals, parents, and healthy siblings, the region of interest was amplified (primer sequences are available upon request). Moreover, to investigate the effects of the candidate variant on the splicing of DOCK2 transcripts, total RNA was isolated from whole blood using the PAXgene Blood RNA Kit (QIAGEN, Hilden, Germany) according to standard procedure. Afterward, cDNA is synthesized by the RevertAid First Strand cDNA Synthesis Kit (ThermoFisher Scientific, Waltham, MA, USA) following the manufacturer's instructions. With the new set primers, which are located in exons 34 and 37 of the *DOCK2* gene, respectively, the region of interest was amplified (primer sequences are available upon request). All amplified fragments were subjected to Sanger sequencing.

Homozygosity Mapping

We utilized PLINK (http://pngu.mgh.harvard.edu/) to extract the runs of homozygosity (ROHs) from the ES data of Family 1 after converting the BAM file to Variant Call Format (VCF). ROH was found using PLINK's ROH algorithm. The PLINK default settings are suitable for detecting large parts of ROH on dense genotyping platforms and remained constant throughout the investigation. By filtering the PLINK output, ROH 4 megabases or less was eliminated [18, 19].

Protein Modeling

The three-dimensional structure of the DOCK2 protein was built by homology modeling using a Swiss-model webserver (https://swissmodel.expasy.org/). As a template, the experimental structure of the human DOCK2 protein (PDB ID: 6TGC), with some missing amino acids, has been retrieved. Visual inspection and graphical representations were performed by the PyMOL (Molecular Graphics System, Version 2.5.7, Schrödinger, LLC).

Flow Cytometric Analysis

Immunophenotyping was performed on EDTA blood samples two hours after venipuncture. The red blood cells were eliminated using a red blood cell lysis buffer, and lymphocytes were stained using monoclonal antibodies against anti-CD3, -CD4, -CD8, -CD16, -CD56, -CD19, -CD20, and -CD27 that were conjugated with fluorochrome dye (Beckman Coulter, CytoFLEX, China). After 30 min of incubation, two PBS washes were performed, and the cells were analyzed using a Cytexpert software flow cytometer. The analysis of the flow cytometric data was carried out using WinMDI software version 2.8.

Functional Assay; Lymphocyte Transformation Test

Using Ficoll/Hypaque gradient centrifugation, peripheral blood mononuclear cells (PBMCs) were collected from sterile, heparinized blood. $1*10^6$ PBMCs were cultured in the polystyrene plate and stimulated with 5µL Bacillus Calmette-Guerin (BCG) and 5µL PHA after being twice washed with RPMI-1640. The cells in the negative control were not stimulated. The cultures were carried out in duplicate and kept for six days at 37 °C in an incubator with 5% carbon dioxide that had been humidified. Cell proliferation was measured using the BrdU proliferation assay kit (Roche, Mannheim, Germany). The stimulation index (SI) was measured as the mean ratio of stimulated

cells' optical density divided by unstimulated cells' optical density. For an assessment of humoral immunity, please see [20].

Dihydrorhodamine Flow Cytometry Assay; Intracellular Production of Hydrogen Peroxide (H_2O_2)

One milliliter of whole blood was obtained from the patient and the healthy control. Lysis buffer was used to lyse the erythrocytes. Following lysis, cells were washed with phosphate-buffered saline (PBS) 1X and resuspended in 1 mL of PBS. Then 200 µL of the cell suspension was added in 5 mL round-bottom polystyrene tubes and maintained at 37 °C in a 5% CO2 incubator during the experiment. To stimulate the production of reactive oxygen species (ROS) on neutrophils and monocytes, 25 µL of 5 µM PMA (Phorbol myristate acetate) solutions were added and incubated at 37 °C for 15 min. Then, 25 µL of 5 mg/mL dihydroergotamine 123 solution (DHR 123) was added to the samples. After the cells were treated for twenty minutes, they were washed with PBS, and a FACSCanto II flow cytometer analyzed the samples to determine the DHR oxidation. The results are presented as an oxidative index in the neutrophil population. The results are presented as a SI.

Results

Clinical Characteristics of IEI Patients with Critical COVID-19

Family 1, Patient 1 (V-3)

The proband, an 8-month-old girl born to consanguineous Iranian parents presented with neonatal cholestasis, congenital CMV infection confirmed by PCR, acute otitis media (AOM), thrombocytopenia, and chronic diarrhea, requiring multiple NICU admissions (Fig. 1A). At four months, she was hospitalized with fever, cough, and shortness of breath, and a chest CT scan revealed multiple ground-glass opacities on both sides and a bronchogenic cyst in the left lung (Fig. 1B), confirmed as COVID-19 by RT-PCR. Despite treatment with vancomycin, piperacillin/tazobactam, ganciclovir, remdesivir, methylprednisolone, and intravenous immunoglobulin (IVIg), her condition deteriorated, leading to ARDS, apnea, and multiple complications, including hepatosplenomegaly, seizures, and periventricular calcifications in the brain, and chronic otitis media (COM) in temporal bone confirmed by CT imaging (Figs. 1C, 1D). Following a brief improvement, she developed thrombocytopenia and EBV infection. The patient died at 13 months of age from thrombocytopenia and acute hemorrhaging prior to the administration of hematopoietic stem cell transplantation. Although COVID-19 increased her susceptibility, thrombocytopenia remained the primary cause of her acute state and death (Please refer to Supplementary File, Section Results, for a detailed report on the patient's clinical timeline and case progression).

Family 1, Patient 2

The older sibling, a male, had congenital CMV and cow's milk protein allergy (CMPA) (confirmed due to rectal bleeding and oral food challenge) and was hospitalized three times in the PICU for COVID-19, with SARS-CoV-2 confirmed each time by RT-PCR. He developed multisystem inflammatory syndrome in children (MIS-C) on two occasions (after 2–3 weeks) and exhibited developmental regression, encephalopathy, and seizures. Imaging revealed diffuse brain atrophy, ventriculomegaly, periventricular calcifications (Fig. 1E), and pansinusitis with otomastoiditis. A chest CT showed an infection in the lungs (Fig. 1F). He also had skin rashes, lymphocytic vasculopathy (Fig. 1G, 1H), and infections, including EBV, enterococcus, and candida. Given the diagnostic criteria observed in the patient, including splenomegaly, persistent fever, elevated ferritin, hypertriglyceridemia, hypofibrinogenemia, and cytopenia, a diagnosis of hemophagocytic lymphohistiocytosis (HLH) was established. Despite comprehensive management, he died at 2 years and 9 months due to arrhythmia and hypoxia (please see the Supplementary file for a detailed case report).

Family 2, Patient 3 (II-2)

The proband, a 26-year-old female, born to non-consanguineous parents (Fig. 1g I), had a history of extensive common and plane warts, bilateral lymphedema, and sensorineural hearing loss (Fig. 1J). A biopsy confirmed verruca vulgaris (Fig. 1K), and a bone marrow biopsy showed myeloid hypoplasia. During the early COVID-19 pandemic, she presented with fever, cough, and hypoxia, with SARS-CoV-2 infection confirmed by RT-PCR. Despite intensive care and ventilatory support, her condition rapidly worsened, and she succumbed to ARDS after four days in the ICU (please see the Supplementary file for a detailed case report).

In summary, in this study, we present three IEI patients who developed severe COVID-19 pneumonia and ultimately succumbed to complications from the infection. The timeline of clinical manifestations for these patients is detailed in Fig. 2, illustrating the progression of their symptoms and the severity of their disease.

Immunological Characteristics of Proband 1 (V-3)

Laboratory findings during the second admission in patient 1 at the age of four months include anemia, lymphopenia,

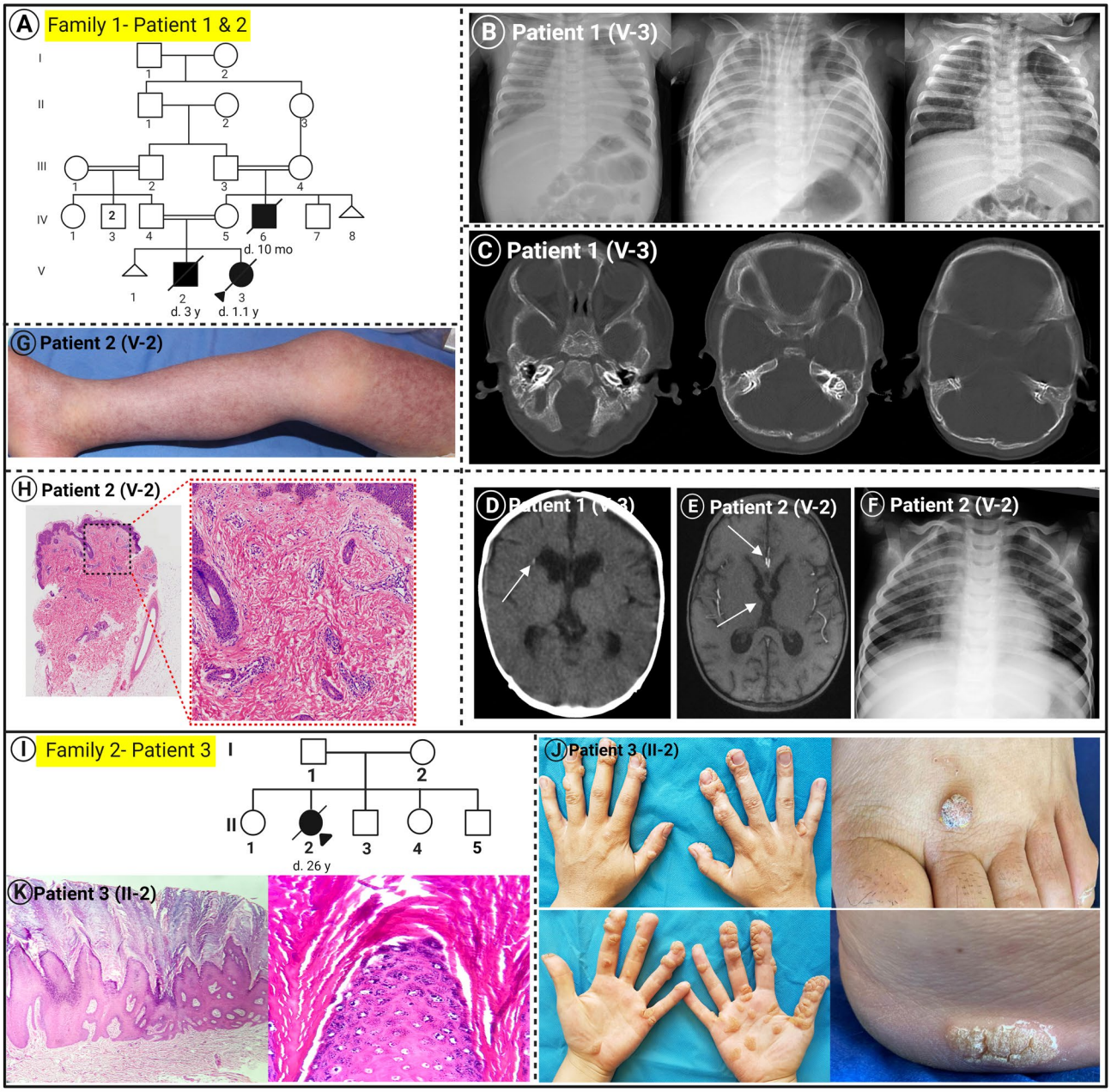

Fig. 1 Family pedigree, clinical manifestations, imaging findings, and histopathology of the patients with DOCK2 deficiency**. (A)** A multiplex consanguineous family affected by several patients with DOCK2 deficiency. **(B)** Chest CT-Scan without contrast demonstrated left lung cystic lesion (bronchogenic cyst), pulmonary infections before COVID infection (left), during COVID infection, and post-COVID infection (right) in proband V-3. **(C)** Temporal bone CT-Scan without contrast demonstrated bilateral chronic otitis media in proband V-3. **(D)** A brain CT scan without contrast demonstrated periventricular calcification in proband V-3. **(E)** MRI imaging without contrast revealed diffuse periventricular calcification and brain atrophy in Patient 2 (V-2). **(F)** A chest CT scan without contrast demonstrated pulmonary infections in Patient 2 (V-2). **(G)** Erythematous skin rash with purpuric hue in Patient 2 (V-2). **(H)** Hematoxylin and eosin (H&E) staining from lesional skin biopsies shows hyperkeratosis, mild spongiosis, acanthosis, and perivascular lymphocytic infiltration (lymphocytic vasculopathy) in Patient 2 (V-2). are seen. **(I)** According to the family's pedigree, there is no evidence of consanguinity or a family history of similar conditions. The proband is identified by an arrowhead. **(J)** Generalized multiple warts were distributed over several anatomical sites in the patient. **(K)** Histopathology of skin lesions showed epidermal hyperplasia, hyperkeratosis, and papillomatosis with the presence of koilocytes in the epidermis consistent with cutaneous wart

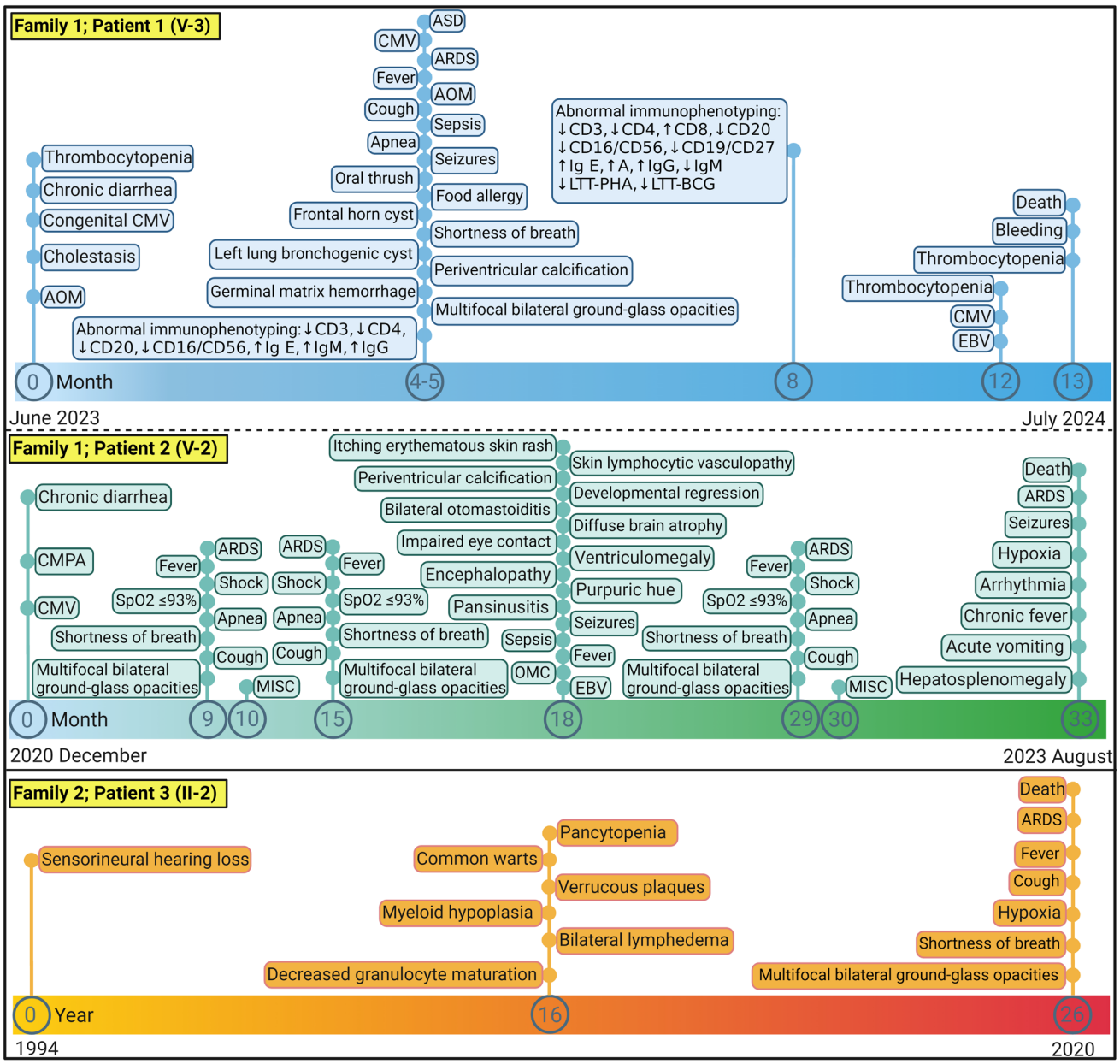

Fig. 2 Timeline of Clinical Manifestations in Patients with *DOCK2* and *GATA2* Pathogenic Variants**.** This schematic figure presents a timeline of clinical manifestations in three patients with GATA2 and DOCK2 mutations. Family 1, Patient 1 (V-3) (blue) is an 8-month-old girl with a *DOCK2* mutation who experienced neonatal cholestasis, CMV infection, and severe COVID-19, ultimately leading to her death at 13 months due to thrombocytopenia and bleeding. Family 1, Patient 2 (V-2) (green) is her older brother, who also had a *DOCK2* pathogenic variant and suffered from repeated COVID-19 infections, MIS-C, severe neurological symptoms, and died at 2 years and 9 months from arrhythmia and hypoxia. Family 2, Patient 3 (II-2) (orange) is a 26-year-old female with a *GATA2* pathogenic variant, who had a history of sensorineural hearing loss, pancytopenia, and HPV-2-related common cutaneous warts, and succumbed to ARDS four days after ICU admission for COVID-19. The timelines illustrate the severe and varied clinical manifestations associated with *DOCK2* and *GATA2* pathogenic variants. AOM, acute otitis media; ARDS, acute respiratory distress syndrome; ASD, atrial septal defect; CMPA, cow's milk protein allergy; CMV, congenital cytomegalovirus; EBV, Epstein-Barr Virus; MIS-C, multisystem inflammatory syndrome in children

decreased CD4 T-helper cells, a CD4/CD8 ratio, and CD3 cells (Figure S1A). She also had increased IgG, IgA, and IgE levels, a slightly increased IgM level, low bilirubin, and high AST (Table S1). When the patient's clinical condition stabilized at eight months of age, we assessed her immunological profile and neutrophil function using respiratory burst tests. The ROS index of V-3 was significantly decreased compared to a control, indicating diminished

H_2O_2 production by neutrophils (Figure S1B). In the lymphocyte transformation test (LTT), phytohemagglutinin (PHA; mitogen) and Bacillus Calmette-Guérin (BCG) responses were impaired, which confirmed the presence of CID (Table S1).

Genetic Dissection of IEI Patients with Life Threatening COVID-19

We performed ES to identify the underlying genetic basis for critical COVID-19 in the DNA of the probands (Patients 1 and 3). We filtered the annotated variants by removing synonymous variants with combined annotation-dependent depletion (CADD) scores < 15 and variants with a minor allele frequency (MAF) of < 0.001.

Family 1: For proband, Patient 1, stepwise filtration reduced the number of putative pathogenic variants to 118 (Fig. 3A). Next, due to familial consanguinity in the pedigree, the ES data were used for single nucleotide variant (SNV)-based homozygosity mapping (HM). The proband's DNA showed 34 ROH > 4 Mb (Fig. 3B). Finally, after removing sequence variants outside of the autozygome of the patient and retaining those variants matched with the patient phenotype, a novel homozygous splicing variant in *DOCK2* (5:170,034,560; c.3624 + 5G > A) within the 7.2 megabase of ROH on 5q35.1 was retained. This sequence variant is located at an evolutionarily conserved nucleotide at the donor splice site of intron 35, as shown by multiple sequence alignments (Figs. 3C and 3D). The predicted consequence of the detected variant was to disturb the donor site at the end of exon 35 (dbscSNV Ada:1, dbscSNV RF:1, and MaxEntScan:7.5) [21, 22]. This sequence variant was present in a population database (gnomAD v4.0.0) with very low frequency in the heterozygous state (0.000006), but it was absent in the homozygous state (Table S2). RT-PCR of cDNA from extracted blood cell mRNA and subsequent Sanger sequencing revealed that exon 35 has been skipped and exon 34 has been spliced to exon 36, which probably produced a frameshift truncated protein (p.L1157Ifs*12) and thus exerted a more severe impact on DOCK2 function (Figs. 3E and 3F). A segregation study with Sanger sequencing in the family showed that both patients were homozygous, and their parents were heterozygous (Fig. 3D). Therefore, based on ES data, the presence of detected homozygous variant inside of ROH, phenotypes of patients, splicing aberration confirmed by cDNA sequencing, and the segregation study of *DOCK2*, we concluded that patients 1 and 2 suffer from DOCK2 deficiency.

Family 2: ES analysis revealed a heterozygous variant in *GATA2*:NM_001145661, c.1075_1102del28, p.W360Sfs*18, which was an out-of-frame 28-bp deletion confirmed by Sanger sequencing (Fig. 4A). This sequence variant was predicted to result in a premature stop codon and nonsense-mediated decay. This variant is not present in the gnomAD database and is predicted to be disease-causing (Table S2). We recently developed a step-wise bioinformatic pipeline for whole-transcriptome-based RNA sequencing (RNA-seq) for the concomitant detection of human genetic and viral determinants of skin lesions in patients with Mendelian disorders. This pipeline combines our virome detection pipeline with the previously developed whole-transcriptome analysis pipeline for pathogenic sequence variants into a single-run experiment [14, 16, 17]. In both the patient's wart and normal-appearing skin samples, Sashimi plots of the RNA-Seq data revealed intra-exonic deletion, which was visualized as an intra-exonic-like splicing pattern in exon 6 of GATA2 mRNA (Fig. 4B). Additionally, the VirPy detected the presence of α-HPV2 with maximum and trivial viral loads in a wart and normal skin biopsies, respectively, compared to no viral load in healthy control skin (Fig. 4C). This gross deletion was located inside the conserved zinc finger type DNA binding domain (349 to 373) of the GATA2 transcription factor (Fig. 4D). Bioinformatic analysis showed that this variant probably produced a frameshift truncated protein (p.W360Sfs*18) (Fig. 4E). The mRNA expression analysis by heatmap showed downregulation of *GATA2* transcript compared with a random set of housekeeping genes in comparison to healthy controls (HC) (n = 4) (Fig. 4F, left panel). The interferon and inflammatory heatmap demonstrates a significant increase in the level of interferon signaling in the skin tissues of GATA2 defective patients in comparison to HCs (n = 4) (Fig. 4F, right panel).

Discussion

Here, we report previously unpublished homozygous and heterozygous pathogenic variants, respectively, in *DOCK2* and *GATA2* patients with a novel phenotype of life-threatening COVID-19 pneumonia. DOCK2 deficiency and GATA2 haploinsufficiency are rare genetic conditions associated with severe immunodeficiency and susceptibility to infections. To date, 35 patients with DOCK2 deficiency have been reported, presenting primarily with recurrent bacterial, viral, and sinopulmonary infections, as well as various immunological abnormalities, such as decreased T and B cell counts and altered immunoglobulin levels. Notably, many of these patients have a consanguineous background and a family history of immunodeficiency. The prognosis for DOCK2 deficiency varies, with about half of the patients surviving, and those who did not undergo hematopoietic stem cell transplantation (HSCT) exhibiting a higher mortality rate [23–38]. In contrast, GATA2 haploinsufficiency, identified in 480 individuals, is the leading monogenic cause of persistent HPV infections, often presenting as refractory warts.

Ⓐ Annotated Variants	Proband
Total number of variants	80183
Exonic/splicing variants	25625
Remove synonymous variants with CADD<15	11925
Homozygous/Compound Heterozygous	5166
Deleterious*, MAF <0.001** and CADD >15	144
Variants in region of homozygosity	11
Variants matching with the phenotype of the patient and segregates within family	*DOCK2*

* FATHMM, MutationAssessor, M-Cap, SIFT, Polyphen2
** gnomAD, ExAC, 1000G, Iranome

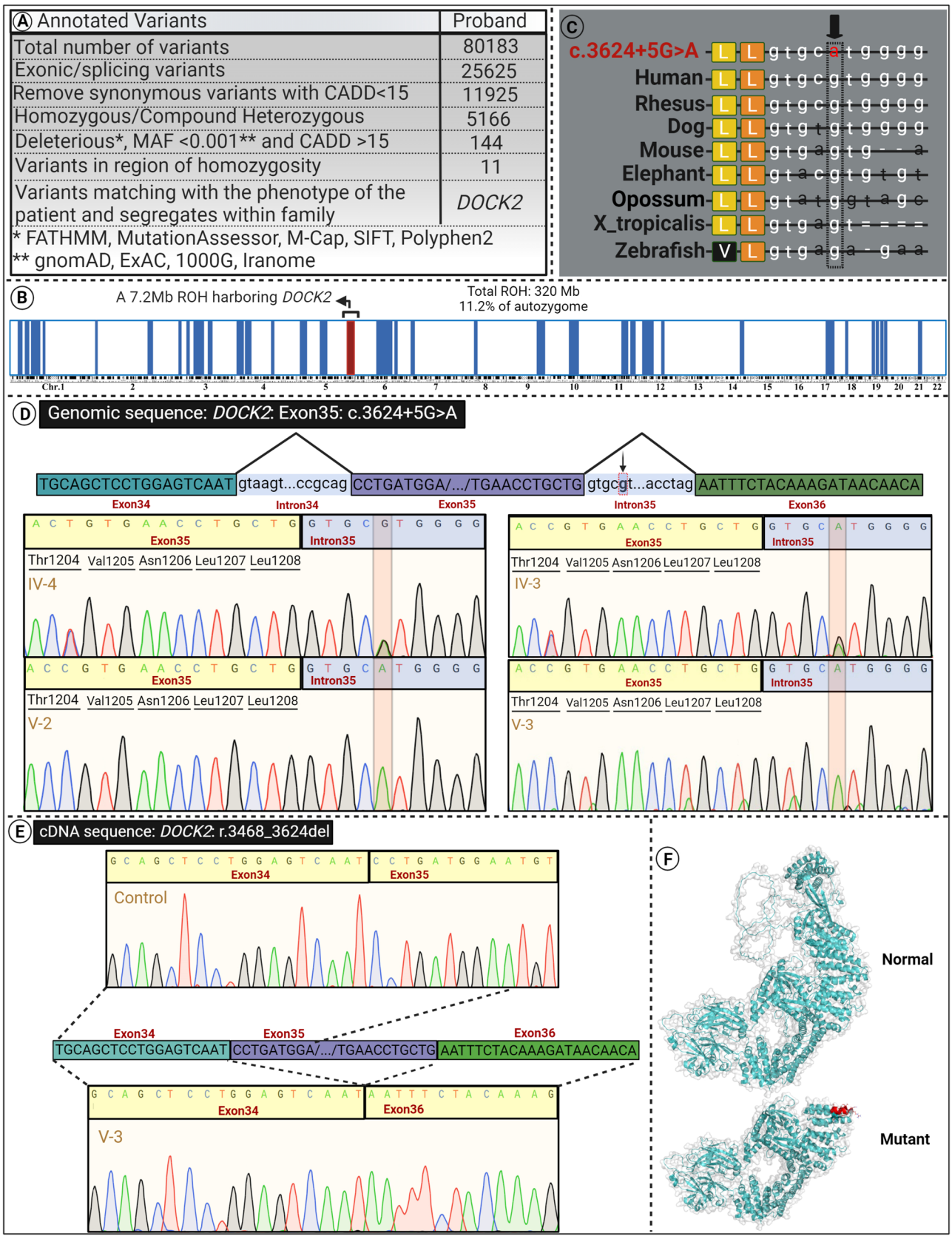

◂**Fig. 3** Detection of a homozygous non-canonical splicing pathogenic variant *DOCK2* in patients 1 and 2**. (A)** Exome sequencing of the DNA of patient 1 revealed 80,183 annotated variants, and bioinformatics filtering by steps shown reduced the number of candidate variants to *DOCK2*. **(B)** Homozygosity mapping revealed 34 regions of homozygosity > 4 Mb, one of them being 7.2 Mb and harboring the *DOCK2* gene locus. The total ROH in the proband is 320 Mb (11.2% of the autozygome), consistent with the presence of extensive consanguinity. **(C)** Conservation analysis showed that the *DOCK2* variant occurred at highly conserved residues through evolution across several species. Black boxes indicate residues that differ from the normal human DOCK2 protein sequence. **(D)** The *DOCK2* splicing variant was confirmed by Sanger sequencing. The parents are heterozygous, and both patients are homozygous for the detected variant. **(E)** The pathogenicity of the variant, leading to exon 35 skipping, was confirmed at the cDNA level by RT-PCR using mRNA isolated from the patient's blood sample. **(F)** The 3D structure of the DOCK2 protein was visualized. The predicted truncated protein as a consequence of skipping an exon was demonstrated. Frameshifted residues are shown in red on the protein structure

EBV is a well-recognized trigger for HLH, particularly in individuals with primary immunodeficiencies that compromise immune regulation, such as DOCK2 deficiency [27, 39]. DOCK2 plays a crucial role in immune cell migration and function, and its deficiency can lead to impaired pathogen clearance and a hyperinflammatory response upon viral infection [23, 40]. In DOCK2-deficient patients, EBV infection can thus drive an unregulated immune response, promoting the development of HLH through sustained activation of T cells and macrophages [27, 40, 41]. Similarly, COVID-19 has been associated with hyperinflammatory syndromes, including HLH, due to dysregulated immune responses that resemble those observed in primary immunodeficiencies [42]. HLH related to a dysregulated inflammatory response post-COVID-19 has been documented in the literature [43–46], and a case of HLH in a patient with DOCK2 deficiency has also been reported [27]. In both DOCK2-deficient patients and COVID-19 patients, the inability to properly control viral infections, such as EBV or SARS-CoV-2, may lead to an overwhelming inflammatory state and predispose individuals to HLH [40, 42]. This convergence of genetic susceptibility (e.g., DOCK2 deficiency) and viral triggers (e.g., EBV, SARS-CoV-2) underscores the importance of immune dysregulation in HLH pathogenesis, emphasizing the critical need for vigilant clinical monitoring and early intervention to potentially mitigate the progression to severe inflammatory states.

While previous reports have noted moderate COVID-19 severity in GATA2-deficient patients, our case is the first to document critical COVID-19 pneumonia in such a patient [47–49]. (For a comprehensive review of the clinical and genetic features of DOCK2 deficiency and GATA2 haploinsufficiency, please see Supplementary File, Figures S2 and S4.)

We speculated that life-threatening COVID-19 pneumonia could be caused by single-gene inborn immunity defects in a subset of patients [50]. From a biological standpoint, discovering this Mendelian subset might be conducive to uncovering other etiologies that disrupt the same physiological mechanisms in other patients in the multifactorial subset [2]. Besides, from a clinical perspective, the ability to dissect this high-risk Mendelian subset from a larger group of patients with multifactorial etiology will provide a framework and justification for incorporating genetic counseling and the genetic diagnostic test into managing life-threatening COVID-19 patients.

In previous reports, by unbiased NGS studies of life-threatening COVID-19 patients, it has emerged that TLR-7-dependent type I and/or III IFN immunity underlies immunity against SARS-CoV-2 [1, 2, 4]. Presumably, critical COVID-19 appears to be caused by the selective disruption of TLR7-dependent blood pDCs type I IFN production. Besides, it has been shown that Dock2 regulates the migration and IFN production of pDCs through the TLR7/9 signaling pathway [4, 23, 51, 52]. Therefore, it is plausible to hypothesize that DOCK2 deficiency through abrogation of TLR7/9-mediated type I IFN induction in pDCs via Rac activation leads to the development of critical COVID pneumonia, although further studies should confirm this. Additionally, the findings of our study align with a recent GWAS of a Japanese cohort, including patients younger than 65 years. A single nucleotide polymorphism (SNP), rs60200309-A, on chromosome 5q35, close to *DOCK2*, was associated with critical COVID-19 [6].

So far, AR single-gene mutations in *TYK2, IRF7, STAT1, STAT2,* and *IRF9* and AD mutations in *TLR3* and *MX1* have been discovered in children with idiopathic severe seasonal influenza pneumonia [4]. The discovery of these rare variants indicates that the disturbance of TLR3-dependent type I and/or type III IFN immunity may be responsible for pneumonia caused by influenza that threatens life. This condition may result from the lack of type I IFN-pDCs in these patients [53]. Patients with monoallelic GATA2 deficiency and susceptibility to severe influenza have also been reported [54]. It was suggested that the absence of type I IFN-producing pDCs, which normally harbor TLR7 to sense influenza virus, in these patients may contribute to the etiology of this severe susceptibility [4, 55, 56]. Patients with GATA2 deficiency are also probably susceptible to hypoxaemic COVID-19 pneumonia, presumably due to a lack of type I IFN-producing pDCs [56, 57].

Collectively, studies of both viral pneumonia cases suggest a shared and, to some extent, overlapping defensive immunity pathway, TLR-7/TLR3-dependent type I and/or III IFN immunity, underlying immunity to both viruses (1, 2, 58). Although ARDS caused by both the seasonal influenza virus and SARS-CoV-2 can be due to mutations that

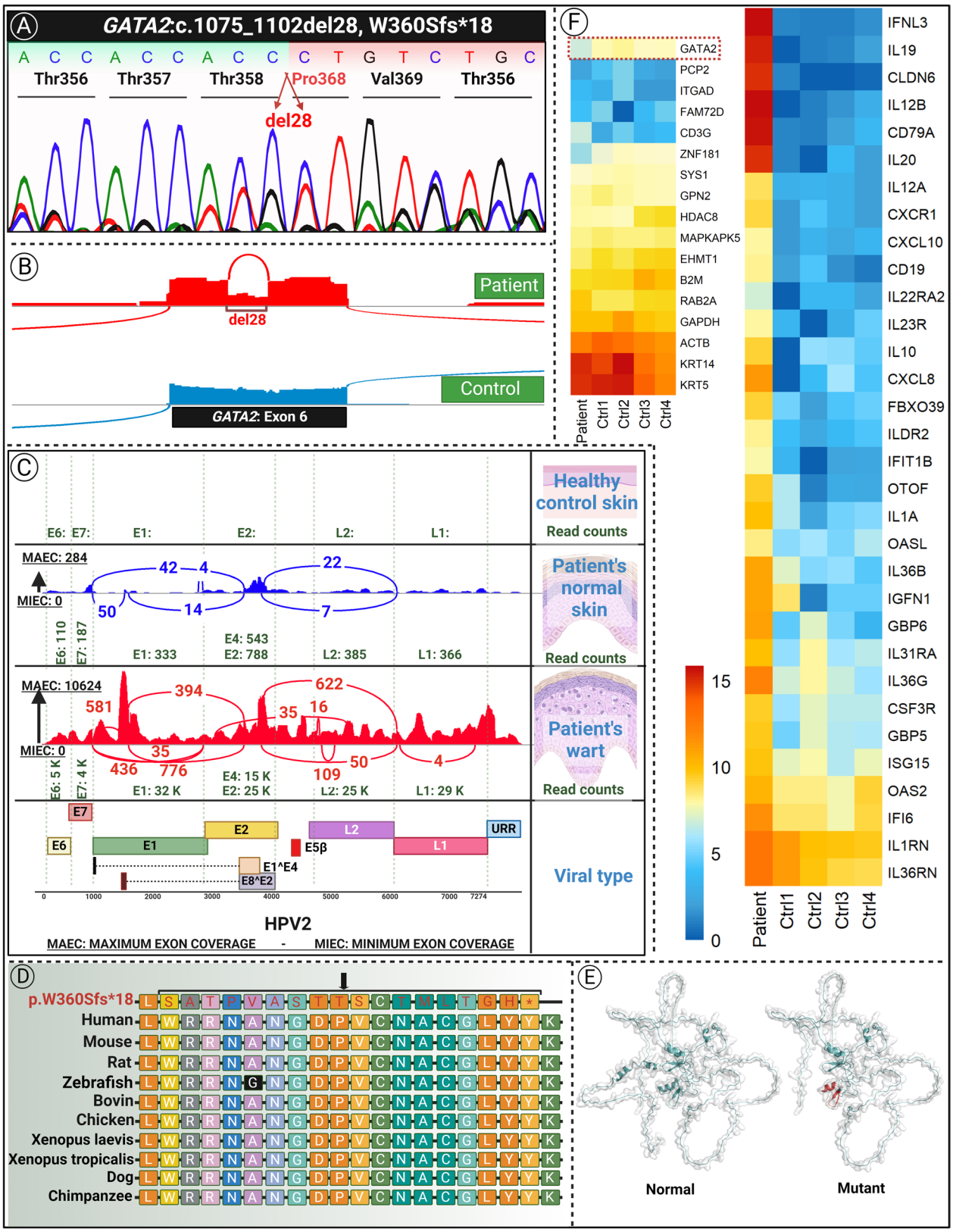
A
GATA2:c.1075_1102del28, W360Sfs*18
A C C A C C A C C C T G T C T G C
Thr356 Thr357 Thr358 Pro368 Val369 Thr356
del28
B
Patient
del28
Control
GATA2: Exon 6
C
Healthy control skin
Read counts
E6: E7: E1: E2: L2: L1:
MAEC: 284
MIEC: 0
42 4 22 50 14 7
E6: 110 E7: 187
E1: 333 E4: 543 E2: 788 L2: 385 L1: 366
Patient's normal skin
Read counts
MAEC: 10624
MIEC: 0
581 394 622 35 16 35 436 776 50 109 4
E6: 5 K E7: 4 K
E1: 32 K E4: 15 K E2: 25 K L2: 25 K L1: 29 K
Patient's wart
Read counts
E7 E2 L2 URR E6 E1 E5β L1 E1^E4 E8^E2
0 1000 2000 3000 4000 5000 6000 7000 7274
Viral type
HPV2
MAEC: MAXIMUM EXON COVERAGE - MIEC: MINIMUM EXON COVERAGE
F
GATA2
PCP2
ITGAD
FAM72D
CD3G
ZNF181
SYS1
GPN2
HDAC8
MAPKAPK5
EHMT1
B2M
RAB2A
GAPDH
ACTB
KRT14
KRT5
Patient Ctrl1 Ctrl2 Ctrl3 Ctrl4
15 10 5 0
IFNL3 IL19 CLDN6 IL12B CD79A IL20 IL12A CXCR1 CXCL10 CD19 IL22RA2 IL23R IL10 CXCL8 FBXO39 ILDR2 IFIT1B OTOF IL1A OASL IL36B IGFN1 GBP6 IL31RA IL36G CSF3R GBP5 ISG15 OAS2 IFI6 IL1RN IL36RN
Patient Ctrl1 Ctrl2 Ctrl3 Ctrl4
D
p.W360Sfs*18 L S A T P V A S T T S C T M L T G H *
Human L W R R N A N G D P V C N A C G L Y Y K
Mouse L W R R N A N G D P V C N A C G L Y Y K
Rat L W R R N A N G D P V C N A C G L Y Y K
Zebrafish L W R R N G N G D P V C N A C G L Y Y K
Bovin L W R R N A N G D P V C N A C G L Y Y K
Chicken L W R R N A N G D P V C N A C G L Y Y K
Xenopus laevis L W R R N A N G D P V C N A C G L Y Y K
Xenopus tropicalis L W R R N A N G D P V C N A C G L Y Y K
Dog L W R R N A N G D P V C N A C G L Y Y K
Chimpanzee L W R R N A N G D P V C N A C G L Y Y K
E
Normal
Mutant

◂**Fig. 4** Genetic etiology and virome study outcomes of a patient with a monoallelic *GATA2* pathogenic variant**. (A)** Sanger sequencing confirmed a heterozygous deletion mutation in *GATA2*:NM_001145661; c.1075_1102del28, p.W360Sfs*18 in the proband. **(B)** The Sashimi plot of RNA-Seq from cutaneous tissue shows the intraexonic 28-nucleotide deletion of exon 6. **(C)** The VirPy detected the presence of α-HPV2 with maximum and minimum viral loads in a wart lesion and apparently normal skin biopsies, respectively, in comparison to no viral load in healthy control skin. **(D)** Conservation analysis showed that the *GATA2* variant occurred at highly conserved residues through evolution across several species. Black boxes indicate residues that differ from the normal human GATA2 protein sequence. **(E)** The 3D structure of the GATA2 protein. The predicted truncated protein as a consequence of deletion was demonstrated. Frameshifted residues are shown in red on the protein structure. **(F)** The mRNA expression analysis (left panel) by heatmap revealed downregulation of *GATA2* transcript (compared with transcripts related to a random set of housekeeping genes) and upregulations of transcripts expressed from interferons and inflammatory gene markers implying strong upregulation of interferon signaling in GATA2 deficient patient compared to healthy controls (n = 4) in biopsied skin tissues (right panel)

impair type I IFN cell-intrinsic immunity in respiratory epithelial cells (RECs), critical COVID-19 seems to be preferentially caused by the selective disruption of TLR7-dependent blood pDCs type I IFN production.

With primary cell material unavailable, analyzing the DOCK2 variant as a recombinant protein could provide insights into its structure and function. Future studies could use this approach to examine its role in immune function for DOCK2 deficiency patients, offering essential data on variant effects without relying on patient-derived samples.

In conclusion, we report novel variants and phenotypes in patients with DOCK2 and GATA2 deficiency. In this research, we broaden the genetic, clinical, and immunological spectrum of DOCK2 deficiency. DOCK2 deficiency has a poor prognosis as a type of CID in individuals who do not receive HSCT, suggesting immediate HSCT as the curative treatment. Further studies are needed to define other treatment options for DOCK2-deficient patients. Moreover, gene therapy could emerge as an additional option in the future.

Supplementary Information The online version contains supplementary material available at https://doi.org/10.1007/s10875-025-01877-z.

Acknowledgements We want to thank our patients, their families, and Dr. Zahra Pourmoghaddas for their collaboration.

Author Contribution S.B., L.Y., A.H.S., M.A.T., B.A.N., E.K., F.V., A.S.M., R.S., F.M., M.S., J.E.G., L.C.T., V.B., E.J., J.L.C., H.V. contributed to study design and/or performed experiments. S.B. and H.V. contributed to writing the original draft. H.H., J.L.C., J.E.G., and F.M., contributed to the review and editing. S.B., B.A.N, R.S., F.M., M.R., H.R., E.K., S.B., M.S., V.H., N.M., S.Z., H.H., V.B., E.J., J.L.C., Q.Z., A.C., H.V. contributed to clinical data and material collection, followed the patient, analyzed data, and clinical care. E.J., J.L.C., and H.V. contributed to funding acquisition. H.H., V.B., E.J., J.L.C., and H.V. contributed to supervision.

Funding The US NIH (grant R01AI143810) and the LEO Foundation (grant LF-OC-22–000965) both supported the authors' studies.

Data Availability The dataset described in this study is available from the corresponding author upon reasonable request.

Declarations

Ethical Approval of Studies This study is in partial fulfillment of S.B. 's PhD thesis, and it was approved by the Ethics Committee of the Isfahan University of Medical Sciences (IR.MUI.MED.REC.1401.255).

Conflicts of Interest Jean-Laurent Casanova serves on the scientific advisory boards of ADMA Biologics Inc., Kymera Therapeutics, and Elixiron Immunotherapeutics. Johann E. Gudjonsson has served as an advisor for Almirall, Eli Lilly, Sanofi, Novartis, BMS, Janssen, Boehringer Ingelheim, and received research grants from Almirall, Prometheus Biosciences, Janssen, Eli Lilly, Boehringer Ingelheim, Galderma. Hakon Hakonarson and Children's Hospital of Philadelphia are equity holders in Nobias Therapeutics, developing MEK inhibitor therapy for complex lymphatic anomalies.
The authors declare no competing interests.
Other authors declare no conflict of interest.

References

1. Casanova J-L, Abel L. Mechanisms of viral inflammation and disease in humans. Science. 2021;374(6571):1080–6.
2. Casanova J-L, Abel L. From rare disorders of immunity to common determinants of infection: Following the mechanistic thread. Cell. 2022;185(17):3086–103.
3. Matuozzo D, Talouarn E, Marchal A, Zhang P, Manry J, Seeleuthner Y, et al. Rare predicted loss-of-function variants of type I IFN immunity genes are associated with life-threatening COVID-19. Genome Med. 2023;15(1):22.
4. Zhang Q. Human genetics of life-threatening influenza pneumonitis. Hum Genet. 2020;139(6–7):941–8.
5. Bastard P, Gervais A, Le Voyer T, Rosain J, Philippot Q, Manry J, et al. Autoantibodies neutralizing type I IFNs are present in~ 4% of uninfected individuals over 70 years old and account for~ 20% of COVID-19 deaths. Science Immunol. 2021;6(62):eabl4340.
6. Namkoong H, Edahiro R, Takano T, Nishihara H, Shirai Y, Sonehara K, et al. DOCK2 is involved in the host genetics and biology of severe COVID-19. Nature. 2022;609(7928):754–60.

7. Niemi ME, Daly MJ, Ganna A. The human genetic epidemiology of COVID-19. Nat Rev Genet. 2022;23(9):533–46.
8. Asano T, Boisson B, Onodi F, Matuozzo D, Moncada-Velez M, Maglorius Renkilaraj MRL, et al. X-linked recessive TLR7 deficiency in~ 1% of men under 60 years old with life-threatening COVID-19. Science Immunol. 2021;6(62):eabl4348.
9. Lévy R, Zhang P, Bastard P, Dorgham K, Melki I, Hadchouel A, et al. Monoclonal antibody-mediated neutralization of SARS-CoV-2 in an IRF9-deficient child. Proc Natl Acad Sci. 2021;118(45):e2114390118.
10. Casanova J-L, Anderson MS. Unlocking life-threatening COVID-19 through two types of inborn errors of type I IFNs. J Clin Invest. 2023;133(3):e166283.
11. Uitto J, Saeidian AH, Youssefian L, Vahidnezhad H. Interpretation of genomic sequence variants in heritable skin diseases: A primer for clinicians. J Am Acad Dermatol. 2023;89(3):569–76.
12. Youssefian L, Vahidnezhad H, Saeidian AH, Mahmoudi H, Karamzadeh R, Kariminejad A, et al. A novel autosomal recessive GJB2-associated disorder: ichthyosis follicularis, bilateral severe sensorineural hearing loss, and punctate palmoplantar keratoderma. Hum Mutat. 2019;40(2):217–29.
13. Saeidian AH, Youssefian L, Vahidnezhad H, Uitto J. Research techniques made simple: whole-transcriptome sequencing by RNA-seq for diagnosis of monogenic disorders. Journal of Investigative Dermatology. 2020;140(6):1117–26. e1.
14. Youssefian L, Saeidian AH, Palizban F, Bagherieh A, Abdollahimajd F, Sotoudeh S, et al. Whole-transcriptome analysis by RNA sequencing for genetic diagnosis of mendelian skin disorders in the context of consanguinity. Clin Chem. 2021;67(6):876–88.
15. Youssefian L, Saeidian AH, Saffarian Z, Ariamanesh M, Abdollahimajd F, Molkara S, et al. Whole-transcriptome Sequencing-Based Profiling of the Cutaneous Virome in Patients with Secondary Immunodeficiency. JID Innovations. 2024:100278.
16. Saeidian AH, Youssefian L, Naji M, Mahmoudi H, Barnada SM, Huang C, et al. Whole transcriptome–based skin virome profiling in typical epidermodysplasia verruciformis reveals α-, β-, and γ-HPV infections. JCI insight. 2023;8(5):e162558.
17. Saeidian AH, Youssefian L, Huang CY, Palizban F, Naji M, Saffarian Z, et al. Whole-transcriptome sequencing–based concomitant detection of viral and human genetic determinants of cutaneous lesions. JCI insight. 2022;7(8):e156021.
18. Vahidnezhad H, Youssefian L, Jazayeri A, Uitto J. Research techniques made simple: genome-wide homozygosity/autozygosity mapping is a powerful tool for identifying candidate genes in autosomal recessive genetic diseases. J Investig Dermatol. 2018;138(9):1893–900.
19. Vahidnezhad H, Youssefian L, Saeidian AH, Zeinali S, Touati A, Abiri M, et al. Genome-wide single nucleotide polymorphism-based autozygosity mapping facilitates identification of mutations in consanguineous families with epidermolysis bullosa. Exp Dermatol. 2019;28(10):1118–21.
20. Youssefian L, Saeidian AH, Tavasoli AR, Kalamati E, Naghipoor K, Hozhabrpour A, et al. Recalcitrant cutaneous warts in a family with inherited ICOS deficiency. J Investig Dermatol. 2022;142(9):2435–45.
21. Yeo G, Burge CB, editors. Maximum entropy modeling of short sequence motifs with applications to RNA splicing signals. J Comput Biol. 2004;11(2-3):377–94.
22. Liu X, Li C, Mou C, Dong Y, Tu Y. dbNSFP v4: a comprehensive database of transcript-specific functional predictions and annotations for human nonsynonymous and splice-site SNVs. Genome Med. 2020;12(1):1–8.
23. Dobbs K, Domínguez Conde C, Zhang S-Y, Parolini S, Audry M, Chou J, et al. Inherited DOCK2 deficiency in patients with early-onset invasive infections. N Engl J Med. 2015;372(25):2409–22.
24. Alizadeh Z, Mazinani M, Shakerian L, Nabavi M, Fazlollahi MR. DOCK2 deficiency in a patient with hyper IgM phenotype. J Clin Immunol. 2018;38:10–2.
25. Alosaimi MF, Shendi H, Beano A, Stafstrom K, El Hawary R, Meshaal S, et al. T-cell mitochondrial dysfunction and lymphopenia in DOCK2-deficient patients. Journal of Allergy and Clinical Immunology. 2019;144(1):306–9. e2.
26. Sharifinejad N, Sadri H, Kalantari A, Delavari S, Noohi A, Aminpour Y, et al. First patient in the Iranian Registry with novel DOCK2 gene mutation, presenting with skeletal tuberculosis, and review of literature. Allergy Asthma Clin Immunol. 2021;17(1):1–8.
27. Aytekin E, ÇAĞDAŞ AYVAZ D, Tan Ç, Cavdarli B, Bilgic I, Tezcan İ. Hematopoietic stem cell transplantation complicated with EBV associated hemophagocytic lymphohistiocytosis in a patient with DOCK2 deficiency. Turk J Pediatr. 2021;63(6):1072–77.
28. Li W, Sun Y, Yu L, Chen R, Gan R, Qiu L, et al. Multiple immune defects in two patients with Novel DOCK2 mutations result in recurrent multiple infection including live attenuated virus vaccine. J Clin Immunol. 2023;43(6):1193–207.
29. Arunachalam AK, Maddali M, Aboobacker FN, Korula A, George B, Mathews V, Edison ES. Primary immunodeficiencies in India: molecular diagnosis and the role of next-generation sequencing. J Clin Immunol. 2021;41:393–413.
30. Moens L, Gouwy M, Bosch B, Pastukhov O, Nieto-Patlàn A, Siler U, et al. Human DOCK2 deficiency: report of a novel mutation and evidence for neutrophil dysfunction. J Clin Immunol. 2019;39:298–308.
31. El Hawary RE, Meshaal SS, Abd Elaziz DS, Alkady R, Lotfy S, Eldash A, et al. Genetic testing in Egyptian patients with inborn errors of immunity: a single-center experience. J Clin Immunol. 2022;42(5):1051–70.
32. Platt CD, Zaman F, Bainter W, Stafstrom K, Almutairi A, Reigle M, et al. Efficacy and economics of targeted panel versus whole-exome sequencing in 878 patients with suspected primary immunodeficiency. J Allergy Clin Immunol. 2021;147(2):723–6.
33. Al-Herz W, Chou J, Delmonte OM, Massaad MJ, Bainter W, Castagnoli R, et al. Comprehensive genetic results for primary immunodeficiency disorders in a highly consanguineous population. Front Immunol. 2019;9:3146.
34. D'Astous-Gauthier K, Desjardins A, Marois L, Falcone EL, Chapdelaine H. DOCK2 deficiency diagnosed 18 years after hematopoietic stem cell transplantation. J Clin Immunol. 2021;41(6):1400–2.
35. Moundir A, Ouair H, Benhsaien I, Jeddane L, Rada N, Amenzoui N, et al. Genetic diagnosis of inborn errors of immunity in an emerging country: A retrospective study of 216 Moroccan patients. J Clin Immunol. 2023;43(2):485–94.
36. Bruusgaard-Mouritsen MA, Masmas T, Borgwardt L, Nazaryan-Petersen L, Heilmann C, Madsen HO, Vibeke MH. A novel DOCK2 variant in siblings with severe combined immunodeficiency. Scand J Immunol. 2023;97(3):e13243.
37. AlKhater SA, Alsaleh MA, Chevalier R, Casanova J-L, Béziat V, Jouanguy E, Zhang S-Y. A Saudi DOCK2-deficient patient with recurrent multiple infections including recalcitrant warts. Res Sq. 2024;Preprint.
38. Vignesh P, Rawat A, Kumrah R, Singh A, Gummadi A, Sharma M, Kaur A. Clinical, immunological, and molecular features of severe combined immune deficiency: a multi-institutional experience from India. Front Immunol. 2020;11:619146.
39. Marsh RA. Epstein-Barr virus and hemophagocytic lymphohistiocytosis. Front Immunol. 2018;8:1902.
40. Ji L, Xu S, Luo H, Zeng F. Insights from DOCK2 in cell function and pathophysiology. Front Mol Biosci. 2022;9:997659.

41. Randall KL, Flesch IE, Mei Y, Miosge LA, Aye R, Yu Z, et al. DOCK2 deficiency causes defects in antiviral T-cell responses and impaired control of herpes simplex virus infection. J Infect Dis. 2024;230(3):e712–21.
42. Thomas D. The virology of hemophagocytic lymphohistiocytosis. In: Shapshak P, editors. Global Virology IV: Viral disease diagnosis and treatment delivery in the 21st Century. 1st ed. Springer; 2024:233–49. https://doi.org/10.1007/978-3-031-57165-7_9.
43. World Health Organisation. Multisystem inflammatory syndrome in children and adolescents with COVID-19. Scientific brief. 2020. https://www.who.int/publications/i/item/multisystem-inflammatory-syndrome-in-children-and-adolescents-with-covid-19.
44. Riphagen S, Gomez X, Gonzalez-Martinez C, Wilkinson N, Theocharis P. Hyperinflammatory shock in children during COVID-19 pandemic. The Lancet. 2020;395(10237):1607–8.
45. Whittaker E, Bamford A, Kenny J, Kaforou M, Jones CE, Shah P, et al. Clinical characteristics of 58 children with a pediatric inflammatory multisystem syndrome temporally associated with SARS-CoV-2. JAMA. 2020;324(3):259–69.
46. Verdoni L, Mazza A, Gervasoni A, Martelli L, Ruggeri M, Ciuffreda M, et al. An outbreak of severe Kawasaki-like disease at the Italian epicentre of the SARS-CoV-2 epidemic: an observational cohort study. The Lancet. 2020;395(10239):1771–8.
47. Biglari S, Moghaddam AS, Tabatabaiefar MA, Sherkat R, Youssefian L, Saeidian AH, et al. Monogenic etiologies of persistent human papillomavirus infections: A comprehensive systematic review. Genet Med. 2024;26(2):101028.
48. Shields AM, Burns SO, Savic S, Richter AG, Anantharachagan A, Arumugakani G, et al. COVID-19 in patients with primary and secondary immunodeficiency: the United Kingdom experience. Journal of Allergy and Clinical Immunology. 2021;147(3):870–5.e1.
49. Meyts I, Bucciol G, Quinti I, Neven B, Fischer A, Seoane E, et al. Coronavirus disease 2019 in patients with inborn errors of immunity: an international study. Journal of Allergy and Clinical Immunology. 2021;147(2):520–31.
50. Casanova J-L, Su HC, Abel L, Aiuti A, Almuhsen S, Arias AA, et al. A global effort to define the human genetics of protective immunity to SARS-CoV-2 infection. Cell. 2020;181(6):1194–9.
51. Gotoh K, Tanaka Y, Nishikimi A, Inayoshi A, Enjoji M, Takayanagi R, et al. Differential requirement for DOCK2 in migration of plasmacytoid dendritic cells versus myeloid dendritic cells. Blood, J Am Soc Hematol. 2008;111(6):2973–6.
52. Gotoh K, Tanaka Y, Nishikimi A, Nakamura R, Yamada H, Maeda N, et al. Selective control of type I IFN induction by the Rac activator DOCK2 during TLR-mediated plasmacytoid dendritic cell activation. J Exp Med. 2010;207(4):721–30.
53. Reizis B. Plasmacytoid dendritic cells: development, regulation, and function. Immunity. 2019;50(1):37–50.
54. Sologuren I, Martínez-Saavedra MT, Solé-Violán J, de Borges de Oliveira Jr E, Betancor E, Casas I, et al. Lethal influenza in two related adults with inherited GATA2 deficiency. J Clin Immunol. 2018;38:513–26.
55. Ciancanelli MJ, Huang SX, Luthra P, Garner H, Itan Y, Volpi S, et al. Life-threatening influenza and impaired interferon amplification in human IRF7 deficiency. Science. 2015;348(6233):448–53.
56. Onodi F, Bonnet-Madin L, Meertens L, Karpf L, Poirot J, Zhang S-Y, et al. SARS-CoV-2 induces human plasmacytoid predendritic cell diversification via UNC93B and IRAK4. J Exp Med. 2021;218(4):e20201387.
57. Zhang Q, Bastard P, Cobat A, Casanova J-L. Human genetic and immunological determinants of critical COVID-19 pneumonia. Nature. 2022;603(7902):587–98.
58. Bastard P, Rosen LB, Zhang Q, Michailidis E, Hoffmann H-H, Zhang Y, et al. Autoantibodies against type I IFNs in patients with life-threatening COVID-19. Science. 2020;370(6515):eabd4585.

Authors and Affiliations

Sajjad Biglari[1] · Leila Youssefian[2] · Mohammad Amin Tabatabaiefar[1] · Amir Hossein Saeidian[3,4] · Bahareh Abtahi-Naeini[5,6] · Erfan Khorram[7] · Roya Sherkat[8] · Atefeh Sohanforooshan Moghaddam[9] · Fatemeh Mohaghegh[10] · Maziyar Rahimi[11] · Hamid Rahimi[12] · Sharareh Babaei[13] · Mohammad Shahrooei[14,15] · Nikoo Mozafari[16] · Shirin Zaresharifi[16] · Fatemeh Vahidnezhad[17] · Vida Homayouni[8] · Lam C. Tsoi[18] · Johann E. Gudjonsson[18] · Hakon Hakonarson[3,19,20] · Jean-Laurent Casanova[21,22,23,24,25] · Emmanuelle Jouanguy[21,22,23] · Vivien Béziat[21,22,23] · Qian Zhang[21,22,23] · Aurélie Cobat[21,22,23] · Hassan Vahidnezhad[3,19,20,26]

✉ Hassan Vahidnezhad
Vahidnezhh@chop.edu

[1] Department of Genetics and Molecular Biology, School of Medicine, Isfahan University of Medical Sciences, Isfahan, Iran

[2] Department of Pathology, Cytogenetics Laboratory, City of Hope National Medical Center, Irwindale, CA, USA

[3] Center for Applied Genomics, Children'S Hospital of Philadelphia, Philadelphia, PA, USA

[4] Department of Molecular and Human Genetics, Baylor College of Medicine, Houston, TX, USA

[5] Pediatric Dermatology Division, Department of Pediatrics, Imam Hossein Children'S Hospital, Isfahan University of Medical Sciences, Isfahan, Iran

[6] Skin Diseases and Leishmaniasis Research Center, Isfahan University of Medical Sciences, Isfahan, Iran

[7] Applied Physiology Research Center, Cardiovascular Research Institute, Isfahan University of Medical Sciences, Isfahan, Iran

[8] Immunodeficiency Diseases Research Center, Isfahan University of Medical Sciences, Isfahan, Iran

[9] Department of Genetics, Faculty of Biological Science, North Tehran Branch, Islamic Azad University, Tehran, Iran

[10] Department of Dermatology, Skin Diseases and Leishmaniasis Research Center, Isfahan University of Medical Sciences, Isfahan, Iran

[11] Pediatrics Department, Isfahan University of Medical Sciences, Isfahan, Iran

[12] Pediatric Infectious Diseases Department, Isfahan University of Medical Sciences, Isfahan, Iran

[13] Department of Asthma, Allergy and Clinical Immunology, Child Growth and Development Research Center, Research Institute of Primordial Prevention of Non-Communicable Disease, Isfahan University of Medical Sciences, Isfahan, Iran

[14] Dr. Shahrooei Laboratory, Tehran, Iran

[15] Clinical and Diagnostic Immunology, 3000 Louvain, KU, Belgium

[16] Skin Research Center, Shahid Beheshti University of Medical Sciences, Tehran, Iran

[17] Department of Computer Science and Engineering Technology, University of Maryland Eastern Shore, Princess Anne, MD, USA

[18] Department of Dermatology, University of Michigan, Ann Arbor, MI 48109, USA

[19] Division of Human Genetics, Children'S Hospital of Philadelphia, Philadelphia, PA, USA

[20] Department of Pediatrics, University of Pennsylvania, Perelman School of Medicine, Philadelphia, PA, USA

[21] St Giles Laboratory of Human Genetics of Infectious Diseases, Rockefeller Branch, Rockefeller University, New York, NY, USA

[22] Laboratory of Human Genetics of Infectious Diseases, Necker Branch, Necker Hospital for Sick Children, Inserm U1163, Paris, France

[23] Imagine Institute, Paris Cité University, Paris, France

[24] Department of Pediatrics, Necker Hospital for Sick Children, Paris, EU, France

[25] Howard Hughes Medical Institute, Chevy Chase, MD 20815, USA

[26] Department of Dermatology, University of Pennsylvania, Perelman School of Medicine, Philadelphia, PA, USA